Acta Cryst E CRYSTALLOGRAPHIC COMMUNICATIONS

ISSN 2056-9890

Synthesis, structure and computational study of *N*-acetyl-*N*′-(4-chlorophenyl)thiourea

Sharatha Kumar[a]* and Tuncer Hökelek[b]

[a]Department of Chemistry, Yenepoya Institute of Arts, Science, Commerce and Management, Mangaluru, Yenepoya University (Deemed to be university), 575013 Karnataka, India, and [b]Hacettepe University, Department of Physics, 06800 Beytepe-Ankara, Türkiye. *Correspondence e-mail: sharathyiascm@yenepoya.edu.in

Received 9 July 2026
Accepted 12 August 2026

Edited by N. Alvarez Failache, Universidad de la Repüblica, Uruguay

Keywords: acetyl; thiourea; 4-chlorophenyl; crystal structure.

Supporting information: this article has supporting information at journals.iucr.org/e

The title compound, $C_9H_9ClN_2OS$, consists of a chlorophenyl ring and acetyl moiety bridged over a thiourea functional group. The dihedral angle between the acetyl group and the planar thiourea group is 1.9 (5)°, and they are oriented at dihedral angles of 57.9 (5) and 59.77 (16)°, respectively, with respect to the phenyl ring. An intramolecular N—H···O hydrogen bond forms an $S(6)$ ring motif. In the crystal, N—H···S and N—H···O hydrogen bonds link the molecules, enclosing $R_2^2(8)$ and $R_2^2(12)$ ring motifs, into infinite chains along the *a*-axis direction. Hirshfeld surface analysis revealed that the most important contributions for crystal packing are H···H (31.1%), H···Cl/Cl···H (16.9%), H···S/S···H (14.4%), H···C/C···H (12.9%) and H···O/O···H (9.4%) interactions. Computational methods revealed N—H···S and N—H···O hydrogen-bonding energies of −13.8 and −10.1 kJ mol^{-1}, respectively. Evaluations of the electrostatic, dispersion and total energy frameworks indicate that the crystal stabilization is dominated by dispersion energy contributions.

1. Chemical context

Acyl thiourea derivatives have attracted considerable attention owing to their biological activities. These compounds have been extensively investigated for their pharmacological potentials, including anticancer properties, where they inhibit cancer cell proliferation and include cytotoxic effects, as well as antimicrobial activities against a broad spectrum of bacterial and fungal pathogens (Cui *et al.*, 2017; Asghar *et al.*, 2018; Asegbeloyin *et al.*, 2018; Saeed *et al.*, 2024; Sakhare *et al.*, 2026). In particular, several thiourea derivatives have demonstrated promising anticancer activities through mechanisms involving enzyme inhibition and interference with tumour cell growth (Cui *et al.*, 2017; Mistry *et al.*, 2017; Ashgar *et al.*, 2018; Zaman *et al.*, 2024; Ramos *et al.*, 2026; Fayyaz *et al.*, 2026).

In addition to their biological relevance, acyl thioureas exhibit interesting conformational preferences and supramolecular behaviours in the solid state. Crystal structures of several 3-acetyl-1-arylthiourea derivatives have been reported (Gowda *et al.*, 2012*d*; Kumar *et al.*, 2012*b*; Shahwar *et al.*, 2012*b*). These compounds typically adopt a pseudo-*anti* conformation with respect to the carbonyl (C═O) and thiocarbonyl (C═S) groups and are commonly feature intramolecular N—H···O hydrogen bonds. In the crystal, N—H···S hydrogen bonds further contribute to the consolidation of the packing arrangement.

As part of our ongoing investigations into acyl thiourea derivatives, we report herein the synthesis, the molecular and crystal structures together with Hirshfeld surface (HS) and

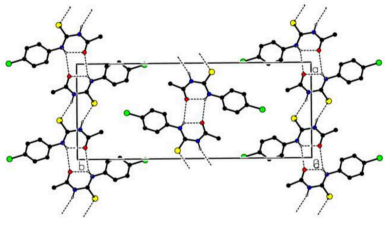

crystal void analyses and interaction energy calculations and energy frameworks of the title compound (**I**).

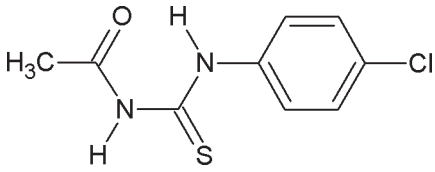

2. Structural commentary

Compound (**I**) consists of a chlorophenyl ring and an acetyl moiety bridged by the thiourea functional group (Fig. 1). The two N—H bonds, beside the thiocarbonyl C=S and carbonyl C=O bonds are in *anti* conformations. The acetyl (O1/C8/C9) group is oriented at a dihedral angle of 1.9 (5)° with respect to the almost planar thiourea (S1/C7/N1/N2) group (r.m.s. deviation = 0.005 Å). The dihedral angles between the phenyl (C1–C6) ring and the acetyl and thiourea groups are 57.9 (5)° and 59.77 (16)°, respectively. The Cl1 and N1 atoms are −0.0638 (19) and 0.027 (5) Å away from the best plane of the phenyl ring. The bond lengths are in normal ranges (Allen *et al.*, 1987) and comparable to those in the similar compounds: *N*-(2-chlorophenyl)-*N*′-propanoylthiourea [(**II**); Kumar & Hökelek, 2026], *N*-(3-chloropropionyl)-*N*′-phenylthiourea [(**III**); Othman *et al.*, 2010] and *N*-(2,6-dimethylphenyl)-*N*′-propanoylthiourea [(**IV**); Yusof *et al.*, 2012], 3-acetyl-1-(2,6-dimethylphenyl)thiourea [(**V**); Kumar *et al.*, 2012*b*], 3-acetyl-1-(2,5-dimethylphenyl)thiourea [(**VI**); Gowda *et al.*, 2012*d*] and 3-acetyl-1-(2-methylphenyl)thiourea [(**VII**); Shahwar *et al.*, 2012*b*]. The C1—N1—C7 [124.8 (5)°] and S1—C7—N1 [125.2 (5)°] bond angles in (**I**) are significantly wider than the corresponding values in (**III**) and (**IV**), while C1—N1—C7 and S1—C7—N1 bond angles are significantly narrower and the same, respectively, when compared with the corresponding values in (**II**). On the other hand, S1—C7—N1 and O1—C8—C9 [123.9 (6)°] bond angles in (**I**) are significantly wider than the corresponding values in (**V**), (**VI**) and (**VII**), while N2—C8—O1 [121.8 (6)°] and S1—C7—N2 [117.9 (5)°] bond angles are significantly narrower, when compared with the corresponding values in (**V**), (**VI**) and (**VII**). An intramolecular N—H···O hydrogen bond (Table 1) in (**I**) forms an *S*(6) ring motif (Etter *et al.*, 1990) (Fig. 1).

Table 1
Hydrogen-bond geometry (Å, °).

D—H···*A*	*D*—H	H···*A*	*D*···*A*	*D*—H···*A*
N1—H1*N*···O1	0.88 (3)	2.04 (6)	2.662 (7)	128 (6)
N1—H1*N*···O1^{i}	0.88 (3)	2.59 (5)	3.319 (7)	141 (6)
N2—H2*N*···S1^{ii}	0.87 (3)	2.54 (3)	3.379 (6)	163 (6)

Symmetry codes: (i) $-x+1, -y+1, z$; (ii) $-x+2, -y+1, z$.

3. Supramolecular features

In the crystal, N—H···S and N—H···O hydrogen bonds (Table 1) link the molecules, enclosing $R_2^2(8)$ and $R_2^2(12)$ ring motifs (Etter *et al.*, 1990), into infinite chains along the *a*-axis direction (Fig. 2). Neither π–π nor C—H···π(ring) interactions are observed.

The intermolecular interactions in the crystal were visualized by carrying out a Hirshfeld surface (HS) analysis using *CrystalExplorer* 17.5 (Spackman *et al.*, 2021). Fig. 3 shows the Hirshfeld surface mapped over $d_{\rm norm}$. The white surface indicates contacts with distances equal to the sum of van der Waals radii, and the red and blue colours indicate distances shorter (in close contact) or longer (distinct contacts) than the van der Waals radii, respectively. The red spots indicate their roles as the respective donor and/or acceptor atoms in hydrogen bonding. They also appear as the blue and red regions corresponding to positive and negative potentials on the HS mapped over electrostatic potential shown in Fig. 4. The blue and red regions indicate positive (hydrogen-bond donors) and negative (hydrogen-bond acceptors) electrostatic potentials.

The overall two-dimensional fingerprint plot is shown in Fig. 5*a* and those delineated into different contact types are illustrated in Fig. 5*b*–*r*, respectively. According to the two-dimensional fingerprint plots, the H···H, H···Cl/Cl···H, H···S/S···H, H···C/C···H and H···O/O···H contacts make

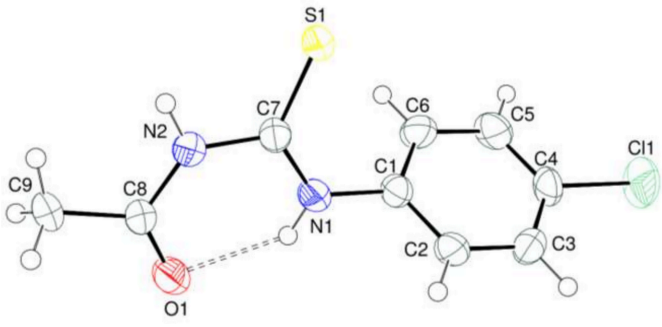

Figure 1
The molecular structure with atom-numbering scheme and 50% probability ellipsoids. The intramolecular N—H···O hydrogen bond is shown as a dashed line.

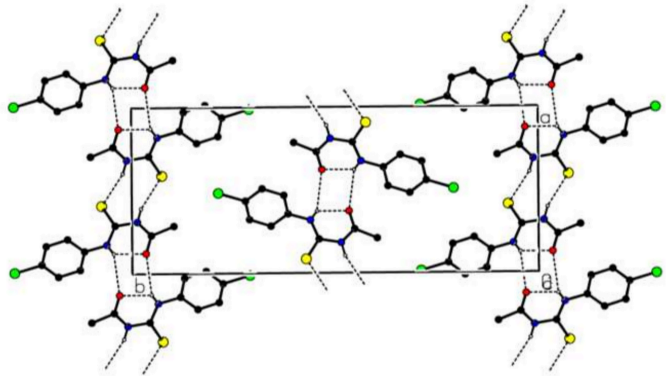

Figure 2
A partial packing diagram viewed down the *c*–axis direction showing the infinite chains along the *a*-axis direction. The intramolecular N—H···O and intermolecular N—H···S and N—H···O hydrogen bonds, which form S(6), $R_2^2(8)$ and $R_2^2(12)$ ring motifs, are shown as dashed lines.

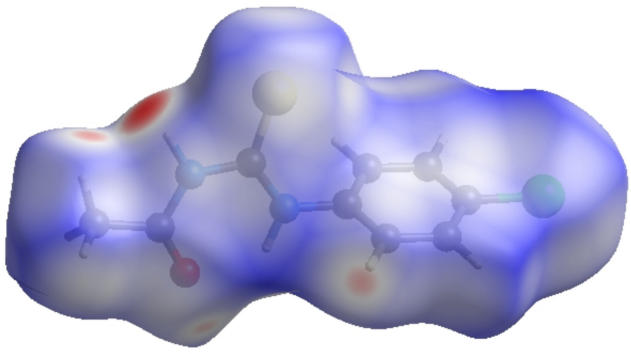

Figure 3
View of the three-dimensional Hirshfeld surface plotted over d_{norm} in the range −0.3415 to 1.2606 a.u.

the most significant contributions to the HS, at 31.1%, 16.9%, 14.4%, 12.9% and 9.4%, respectively (Fig. 5). In *N*-(2-chlorophenyl)-*N*′-propanoylthiourea [(**II**); Kumar & Hökelek, 2026], the most important contributions for the crystal packing are H···H (39.2%), H···Cl/Cl···H (15.8%), H···S/S···H (14.2%) and H···C/C··· H (9.9%) interactions.

The volume of the crystal voids (Fig. 6*a*,*b*) and the percentage of free space in the unit cell were calculated to be 87.5 Å^3 and 8.6%, respectively. Thus, the crystal packing appears compact and the mechanical stability should be substantial. In compound (**II**), the volume of the crystal voids and the percentage of free space in the unit cell were calculated to be 105.62 Å^3 and 9.33%, respectively, showing that there was no large cavity in the crystal packing.

The intermolecular interaction energies were calculated using CE–B3LYP/6–31G(d,p) energy model available in *CrystalExplorer* 17.5 (Spackman *et al.*, 2021), where a cluster of molecules is generated by applying crystallographic symmetry operations with respect to a selected central molecule within the radius of 3.8 Å by default. The total intermolecular energy (E_{tot}) is the sum of electrostatic (E_{ele}), polarization (E_{pol}), dispersion (E_{dis}) and exchange-repulsion (E_{rep}) energies (Turner *et al.*, 2015) with scale factors of 1.057, 0.740, 0.871 and 0.618, respectively (Mackenzie *et al.*, 2017).

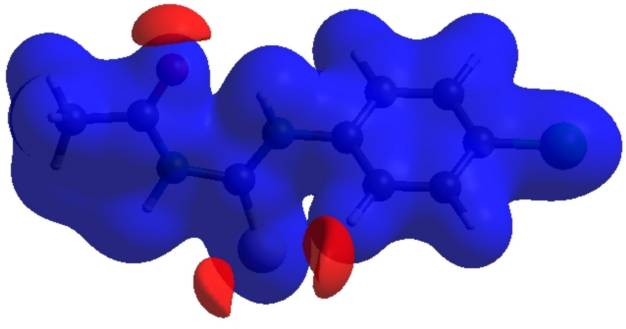

Figure 4
View of the three-dimensional Hirshfeld surface of the title compound plotted over electrostatic potential in the range of −0.0500 to 0.0500 a.u. using the STO-3 G basis set at the Hartree–Fock level of theory. Hydrogen-bond donors and acceptors are shown as blue and red regions around the atoms, corresponding to positive and negative potentials, respectively.

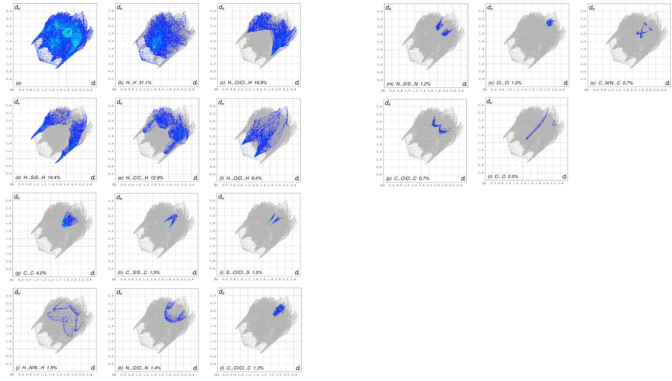

Figure 5
The full two-dimensional fingerprint plots for title molecule, showing (*a*) all interactions, and delineated into (*b*) H···H, (*c*) H···Cl/Cl···H, (*d*) H···S/S···H, (*e*) H···C/C···H, (*f*) H···O/O···H, (*g*) C···C, (*h*) C···S/S···C, (*i*) S···Cl/Cl···S, (*j*) H···N/N···H, (*k*) N···O/O···N, (*l*) C···Cl/Cl···C, (*m*) N···S/S···N, (*n*) Cl···Cl, (*o*) C···N/N···C, (*p*) C···O/O···C and (*r*) O···O interactions. The d_i and d_e values are the closest internal and external distances (in Å) from given points on the Hirshfeld surface.

Hydrogen-bonding interaction energies (in kJ mol^{-1}) were calculated to be −9.1 (E_{ele}), −1.4 (E_{pol}), −6.6 (E_{dis}), 4.3 (E_{rep}) and −13.8 (E_{tot}) for the N2—H2*N*···S1 and −4.5 (E_{ele}), −1.4 (E_{pol}), −10.8 (E_{dis}), 8.3 (E_{rep}) and −10.1 (E_{tot}) for the N1—H1*N*···O1 hydrogen-bonding interactions (see supporting information).

Energy frameworks combine the calculation of intermolecular interaction energies with a graphical representation of their magnitudes, and were constructed for E_{ele} (red cylinders), E_{dis} (green cylinders) and E_{tot} (blue cylinders) (Fig. 7*a*,*b*,*c*). Evaluation of the electrostatic, dispersion and

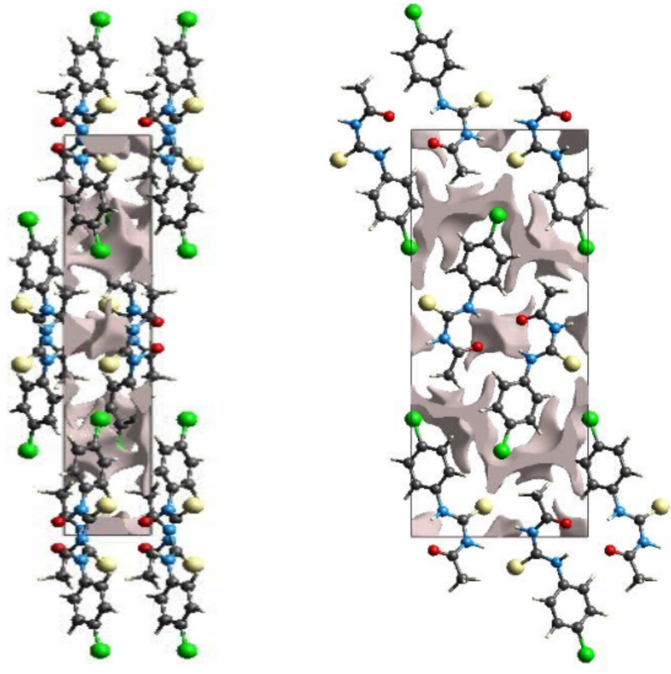

Figure 6
Crystal voids viewed down the (*a*) *a*-axis and (*b*) *c*-axis directions.

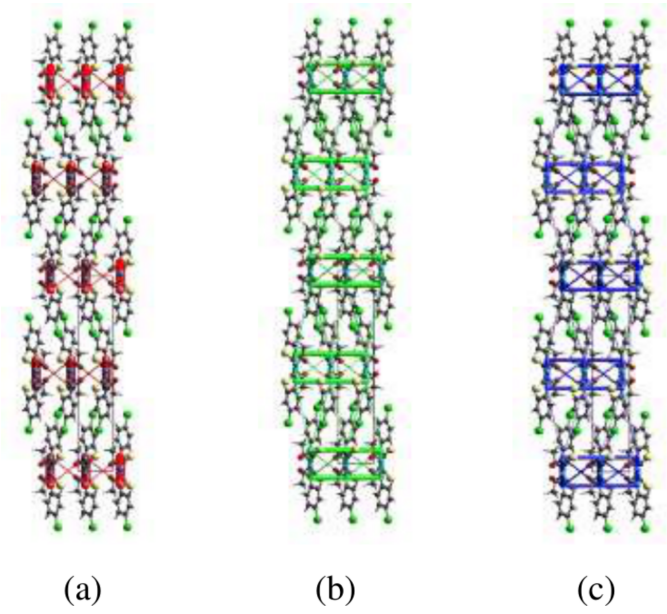

Figure 7
The energy frameworks for a cluster of molecules, viewed down the *a* axis, showing the (*a*) electrostatic energy, (*b*) dispersion energy and (*c*) total energy diagrams. The cylindrical radius is proportional to the relative strength of the corresponding energies and they were adjusted to the same scale factor of 80 with cut-off value of 5 kJ mol^{-1} within 2 × 2 × 2 unit cells.

total energy frameworks indicates that the stabilization of the crystal structure is dominated by the dispersion energy contributions.

4. Database survey

A search of the Cambridge Structural Database (CSD, Version 6.00, updated May 2025; Groom *et al.*, 2016) revealed eleven closely related structures of *N*-acetyl-*N*′-arylthiourea derivatives: 3-acetyl-1-phenylthiourea, $C_9H_{10}N_2OS$ (CSD refcode GARBIM; Shahwar *et al.*, 2012*a*), 3-acetyl-1-(2-methylphenyl)thiourea, $C_{10}H_{12}N_2OS$ (CSD refcode YAXNUI; Shahwar *et al.*, 2012*b*), 3-acetyl-1-(3-chlorophenyl)-thiourea, $C_9H_9ClN_2OS$ (YAXTIC; Shahwar *et al.*, 2012*c*), 3-acetyl-1-(3-methylphenyl)thiourea, $C_{10}H_{12}N_2OS$ (LEGQEV; Gowda *et al.*, 2012*a*), 3-acetyl-1-(4-methylphenyl)thiourea, $C_{10}H_{12}N_2OS$ (XAZYOO; Gowda *et al.*, 2012*b*), 3-acetyl-1-(2,4-dimethylphenyl)thiourea, $C_{11}H_{14}N_2OS$ (LEGCIL; Gowda *et al.*, 2012*c*), 3-acetyl-1-(2,5-dimethylphenyl)thiourea, $C_{11}H_{14}N_2OS$ (LEDYAW; Gowda *et al.*, 2012*d*), 3-acetyl-1-(2,3-dichlorophenyl)thiourea, $C_9H_8Cl_2N_2OS$ (LEFBEF; Gowda *et al.*, 2012*e*), 3-acetyl-1-(2,3-dimethylphenyl)thiourea, $C_{11}H_{14}N_2OS$ (XEBKUM; Kumar *et al.*, 2012*a*), 3-acetyl-1-(2,6-dimethylphenyl)thiourea, $C_{11}H_{14}N_2OS$ (Kumar *et al.*, 2012*b*), 3-acetyl-1-(2,6-dichlorophenyl)thiourea, $C_9H_8Cl_2N_2OS$ (CLEDSUK; Kumar *et al.*, 2012*c*). Overall, these *N*-acetyl-*N*′-arylthiourea derivatives consistently exhibit hydrogen-bonding networks dominated by N—H···S and N—H···O interactions, which frequently generate graph-set motifs such as $R_2^2(8)$ and $R_2^2(12)$, and assemble the molecules into one-, two- or three-dimensional supramolecular architectures. In several structures, three-centre N—H···(O,S) hydrogen bonds and weaker C—H···S contacts further reinforce the crystal packing, highlighting the key role of hydrogen bonding in consolidating this family of compounds.

5. Synthesis and crystallization

The title compound was synthesized by adding a solution of acetyl chloride (0.10 mol) in acetone (30 ml) dropwise to a suspension of potassium thiocyanate (0.10 mol) in acetone (30 ml), and then stirred for 2 h. Then, the reaction mixture was refluxed for 30 min. After cooling to room temperature, a solution of 4-chloroaniline (0.10 mol) in acetone (10 ml) was added and the solution refluxed for 3 h. After completion of the reaction (monitored by TLC), the reaction mixture was poured into acidified cold water. The solids separated were filtered under suction, washed thoroughly with water and dried under vacuum. Colourless crystals suitable for X-ray analysis were obtained by slow evaporation of an acetonitrile solution. White solid, yield 85%, m.p. 445 K. IR (KBr) cm^{-1}: 3181 (N—H str.), 1164 (C═S str.) and 1690 (C═O str.).

6. Refinement

Crystal data, data collection and structure refinement details are summarized in Table 2. The NH hydrogen atoms were located from a difference-Fourier map and refined isotropically. The C-bound hydrogen-atom positions were calculated geometrically at distances of 0.93 Å (for aromatic CH) and 0.96 Å (for methyl CH) and refined using a riding model with $U_{iso}(H) = k \times U_{eq}$ (C, N), where k = 1.5 for methyl hydrogens and k = 1.2 for other H atoms.

Acknowledgements

The authors thank the Yenepoya Deemed to be University for the facilities and financial support. TH is also grateful to Hacettepe University Scientific Research Project Unit (grant No. 013 D04 602 004). The authors' contributions are as follows. Conceptualization, SK and TH; synthesis, SK; X-ray analysis, SK and TH; Hirshfeld surface analysis, TH; writing (review and editing of the manuscript) SK and TH; supervision, TH and SK.

References

Allen, F. H., Kennard, O., Watson, D. G., Brammer, L., Orpen, A. G. & Taylor, R. (1987). *J. Chem. Soc. Perkin Trans. 2* pp. S1–S19.
Asegbeloyin, J. N., Oyeka, E. E., Okpareke, O. & Ibezim, A. (2018). *J. Mol. Struct.* **1153**, 69–77.
Asghar, F., Rana, S., Fatima, S., Badshah, A., Lal, B. & Butler, I. S. (2018). *New J. Chem.* **42**, 7154–7165.
Cui, P., Li, X., Zhu, M., Wang, B., Liu, J. & Chen, H. (2017). *Bioorg. Med. Chem. Lett.* **27**, 2234–2237.
Etter, M. C., MacDonald, J. C. & Bernstein, J. (1990). *Acta Cryst.* B**46**, 256–262.
Farrugia, L. J. (2012). *J. Appl. Cryst.* **45**, 849–854.

Fayyaz, A., Ejaz, S. A., Ahmed, A., Channar, P. A., Afzal, S., Ujan, R., Saeed, A., Bibi, R., Alsfouk, B. A., Abbas, Q., Sahito, R., Bolte, M. & Hökelek, T. (2026). *Biosci. Rep.* **46**, BSR20253519.
Gowda, B. T., Foro, S. & Kumar, S. (2012*a*). *Acta Cryst.* E**68**, o2574.
Gowda, B. T., Foro, S. & Kumar, S. (2012*b*). *Acta Cryst.* E**68**, o2128.
Gowda, B. T., Foro, S. & Kumar, S. (2012*c*). *Acta Cryst.* E**68**, o2498.
Gowda, B. T., Foro, S. & Kumar, S. (2012*d*). *Acta Cryst.* E**68**, o2338.
Gowda, B. T., Foro, S. & Kumar, S. (2012*e*). *Acta Cryst.* E**68**, o2353.
Groom, C. R., Bruno, I. J., Lightfoot, M. P. & Ward, S. C. (2016). *Acta Cryst.* B**72**, 171–179.
Kumar, S., Foro, S. & Gowda, B. T. (2012*a*). *Acta Cryst.* E**68**, o2191.
Kumar, S., Foro, S. & Gowda, B. T. (2012*b*). *Acta Cryst.* E**68**, o2306.
Kumar, S., Foro, S. & Gowda, B. T. (2012*c*). *Acta Cryst.* E**68**, o2307.
Kumar, S. & Hökelek, T. (2026). *Acta Cryst.* E**82**, 816–820.
Mackenzie, C. F., Spackman, P. R., Jayatilaka, D. & Spackman, M. A. (2017). *IUCrJ* **4**, 575–587.
Mistry, B. M., Shin, H. S., Pandurangan, M. & Patel, R. V. (2017). *J. Chem. Res.* **41**, 598–602.
Othman, E. A., Soh, S. K. C. & Yamin, B. M. (2010). *Acta Cryst.* E**66**, o628.
Oxford Diffraction (2009). *CrysAlis CCD* and *CrysAlis RED*. Oxford Diffraction Ltd, Abingdon, England.
Parsons, S., Flack, H. D. & Wagner, T. (2013). *Acta Cryst.* B**69**, 249–259.
Ramos, R., Plutín, A. M., Mocelo, R. O., DJukic, J. P., Pinto, C. B., Castellano, E. E., Echeverría, G. A., Piro, O. E., Erben, M. F., Colina-Vegas, L., Cunha, B. N. & Batista, A. A. (2026). *J. Inorg. Biochem.* **276**, 113180.
Saeed, A., Ahmed, A., Haider, M. B., Ismail, H., Hayat, K., Shabir, G. & El-Seedi, H. R. (2024). *RSC Adv.* **14**, 1018–1033.
Sakhare, N., Joshi, P., Bhoye, M., Kharad, K., Mhaske, P., Takate, S. & Mhaske, S. (2026). *ChemistrySelect* **11**, e06812.
Shahwar, D., Tahir, M. N., Chohan, M. M., Ahmad, N. & Raza, M. A. (2012*b*). *Acta Cryst.* E**68**, o1160–o1160.
Shahwar, D., Tahir, M. N., Chohan, M. M., Ahmad, N. & Raza, M. A. (2012*c*). *Acta Cryst.* E**68**, o1189–o1189.
Shahwar, D., Tahir, M. N., Chohan, M. M., Ahmad, N. & Samiullah (2012*a*). *Acta Cryst.* E**68**, o508–o508.
Sheldrick, G. M. (2015*a*). *Acta Cryst.* A**71**, 3–8.
Sheldrick, G. M. (2015*b*). *Acta Cryst.* C**71**, 3–8.
Spackman, P. R., Turner, M. J., McKinnon, J. J., Wolff, S. K., Grimwood, D. J., Jayatilaka, D. & Spackman, M. A. (2021). *J. Appl. Cryst.* **54**, 1006–1011.
Spek, A. L. (2020). *Acta Cryst.* E**76**, 1–11.
Turner, M. J., Thomas, S. P., Shi, M. W., Jayatilaka, D. & Spackman, M. A. (2015). *Chem. Commun.* **51**, 3735–3738.

Table 2
Experimental details.

Crystal data	
Chemical formula	$C_9H_9ClN_2OS$
M_r	228.69
Crystal system, space group	Orthorhombic, $P2_12_12$
Temperature (K)	293
a, b, c (Å)	10.090 (3), 24.830 (6), 4.079 (2)
V (Å^3)	1021.9 (6)
Z	4
Radiation type	Mo $K\alpha$
μ (mm^{-1})	0.54
Crystal size (mm)	0.50 × 0.08 × 0.06
Data collection	
Diffractometer	Oxford Diffraction Xcalibur with Sapphire CCD
Absorption correction	Multi-scan (*CrysAlis RED*; Oxford Diffraction, 2009)
T_{min}, T_{max}	0.772, 0.968
No. of measured, independent and observed [$I > 2\sigma(I)$] reflections	2960, 1803, 1527
R_{int}	0.018
(sin $\theta/\lambda)_{max}$ (Å^{-1})	0.613
Refinement	
$R[F^2 > 2\sigma(F^2)]$, $wR(F^2)$, S	0.060, 0.152, 1.26
No. of reflections	1803
No. of parameters	134
No. of restraints	2
H-atom treatment	H atoms treated by a mixture of independent and constrained refinement
$\Delta\rho_{max}$, $\Delta\rho_{min}$ (e Å^{-3})	0.63, −0.28
Absolute structure	Flack x determined using 495 quotients $[(I^+)-(I^-)]/[(I^+)+(I^-)]$ (Parsons et al., 2013), 672 Friedel pairs
Absolute structure parameter	0.54 (5)

Computer programs: *CrysAlis CCD* and *CrysAlis RED* (Oxford Diffraction, 2009), *SHELXT2013/1* (Sheldrick, 2015*a*), *SHELXL2014/6* (Sheldrick, 2015*b*), *ORTEP-3 for Windows* and *WinGX* publication routines (Farrugia, 2012) and *PLATON* (Spek, 2020).

Yusof, M. S. M., Mutalib, S. F. A., Arshad, S. & Razak, I. A. (2012). *Acta Cryst.* E**68**, o982.
Zaman, H., Saeed, A., Ismail, H., Anwaar, S., Latif, M., Hashmi, M. Z. & El-Seedi, H. R. (2024). *RSC Adv.* **14**, 33235–33246.

supporting information

Acta Cryst. (2026). E**82**, 1066-1070 [https://doi.org/10.1107/S2056989026008315]

Synthesis, structure and computational study of *N*-acetyl-*N*′-(4-chlorophenyl)-thiourea

Sharatha Kumar and Tuncer Hökelek

Computing details

N-Acetyl-*N*′-(4-chlorophenyl)thiourea

Crystal data

$C_9H_9ClN_2OS$
$M_r = 228.69$
Orthorhombic, $P2_12_12$
$a = 10.090$ (3) Å
$b = 24.830$ (6) Å
$c = 4.079$ (2) Å
$V = 1021.9$ (6) Å^3
$Z = 4$
$F(000) = 472$
$D_x = 1.486$ Mg m^{-3}
Mo $K\alpha$ radiation, $\lambda = 0.71073$ Å
Cell parameters from 1233 reflections
$\theta = 3.2$–$28.0°$
$\mu = 0.54$ mm^{-1}
$T = 293$ K
Needle, colourless
0.50 × 0.08 × 0.06 mm

Data collection

Oxford Diffraction Xcalibur with Sapphire CCD diffractometer
Rotation method data acquisition using ω scans.
Absorption correction: multi-scan (CrysAlis RED; Oxford Diffraction, 2009)
$T_{min} = 0.772$, $T_{max} = 0.968$
2960 measured reflections
1803 independent reflections
1527 reflections with $I > 2\sigma(I)$
$R_{int} = 0.018$
$\theta_{max} = 25.8°$, $\theta_{min} = 2.6°$
$h = -12 \rightarrow 7$
$k = -30 \rightarrow 27$
$l = -4 \rightarrow 4$

Refinement

Refinement on F^2
Least-squares matrix: full
$R[F^2 > 2\sigma(F^2)] = 0.060$
$wR(F^2) = 0.152$
$S = 1.26$
1803 reflections
134 parameters
2 restraints
Hydrogen site location: mixed
H atoms treated by a mixture of independent and constrained refinement
$w = 1/[\sigma^2(F_o^2) + (0.0725P)^2 + 0.5752P]$ where $P = (F_o^2 + 2F_c^2)/3$
$(\Delta/\sigma)_{max} < 0.001$
$\Delta\rho_{max} = 0.63$ e Å^{-3}
$\Delta\rho_{min} = -0.28$ e Å^{-3}
Absolute structure: Flack *x* determined using 495 quotients $[(I^+)-(I^-)]/[(I^+)+(I^-)]$ (Parsons et al., 2013), 672 Friedel pairs.
Absolute structure parameter: 0.54 (5)

Special details

Geometry. All esds (except the esd in the dihedral angle between two l.s. planes) are estimated using the full covariance matrix. The cell esds are taken into account individually in the estimation of esds in distances, angles and torsion angles; correlations between esds in cell parameters are only used when they are defined by crystal symmetry. An approximate (isotropic) treatment of cell esds is used for estimating esds involving l.s. planes.

Fractional atomic coordinates and isotropic or equivalent isotropic displacement parameters (Å²)

	x	*y*	*z*	U_{iso}*/U_{eq}
C1	0.6395 (6)	0.3823 (2)	0.2485 (17)	0.0330 (15)
C2	0.5266 (6)	0.3718 (2)	0.4246 (18)	0.0393 (18)
H2	0.4776	0.3999	0.5148	0.047*
C3	0.4861 (6)	0.3184 (2)	0.4666 (19)	0.0415 (15)
H3	0.4082	0.3109	0.5795	0.050*
C4	0.5605 (7)	0.2774 (2)	0.3427 (19)	0.0416 (18)
C5	0.6731 (7)	0.2879 (3)	0.166 (2)	0.0462 (18)
H5	0.7223	0.2597	0.0787	0.055*
C6	0.7133 (7)	0.3404 (3)	0.118 (2)	0.046 (2)
H6	0.7896	0.3477	−0.0020	0.055*
C7	0.7919 (6)	0.4582 (2)	0.2858 (17)	0.0320 (15)
C8	0.7334 (6)	0.5465 (2)	0.023 (2)	0.0386 (16)
C9	0.7889 (6)	0.6019 (2)	−0.022 (2)	0.0418 (17)
H9A	0.8744	0.6041	0.0801	0.063*
H9B	0.7304	0.6278	0.0766	0.063*
H9C	0.7973	0.6095	−0.2519	0.063*
N1	0.6773 (5)	0.4373 (2)	0.1981 (16)	0.0390 (14)
H1N	0.625 (5)	0.454 (2)	0.060 (14)	0.047*
N2	0.8134 (5)	0.5127 (2)	0.2074 (16)	0.0379 (14)
H2N	0.893 (4)	0.522 (2)	0.260 (18)	0.045*
O1	0.6252 (4)	0.53307 (18)	−0.0660 (16)	0.0561 (16)
Cl1	0.5120 (2)	0.21064 (7)	0.4144 (6)	0.0678 (8)
S1	0.91037 (14)	0.42582 (6)	0.4885 (5)	0.0383 (4)

Atomic displacement parameters (Å²)

	U^{11}	U^{22}	U^{33}	U^{12}	U^{13}	U^{23}
C1	0.032 (3)	0.027 (3)	0.039 (4)	−0.003 (2)	−0.006 (3)	0.001 (3)
C2	0.035 (3)	0.026 (3)	0.057 (5)	0.004 (3)	0.003 (3)	−0.001 (3)
C3	0.036 (3)	0.037 (3)	0.051 (5)	−0.003 (3)	0.010 (4)	0.004 (3)
C4	0.046 (4)	0.024 (3)	0.055 (5)	−0.008 (3)	−0.006 (3)	0.008 (3)
C5	0.048 (4)	0.027 (3)	0.063 (5)	0.007 (3)	0.001 (3)	−0.005 (3)
C6	0.033 (4)	0.034 (3)	0.070 (6)	0.001 (3)	0.005 (3)	−0.001 (3)
C7	0.033 (3)	0.029 (3)	0.034 (4)	0.000 (3)	0.002 (3)	0.003 (3)
C8	0.033 (3)	0.027 (3)	0.055 (5)	0.000 (2)	0.004 (4)	0.007 (3)
C9	0.044 (4)	0.024 (3)	0.058 (5)	0.002 (3)	−0.001 (4)	0.007 (3)
N1	0.032 (3)	0.028 (3)	0.057 (4)	0.001 (2)	−0.005 (3)	0.006 (2)
N2	0.030 (3)	0.030 (3)	0.053 (4)	−0.002 (2)	−0.002 (3)	0.004 (2)
O1	0.040 (3)	0.035 (2)	0.093 (5)	−0.002 (2)	−0.019 (3)	0.012 (3)

Cl1	0.0788 (14)	0.0269 (8)	0.098 (2)	−0.0128 (9)	0.0097 (12)	0.0051 (9)
S1	0.0337 (7)	0.0301 (7)	0.0511 (11)	−0.0010 (6)	−0.0045 (9)	0.0102 (8)

Geometric parameters (Å, º)

C1—C2	1.372 (9)	C7—N1	1.317 (8)
C1—C6	1.386 (9)	C7—N2	1.406 (8)
C1—N1	1.433 (8)	C7—S1	1.661 (6)
C2—C3	1.398 (8)	C8—O1	1.198 (7)
C2—H2	0.9300	C8—N2	1.385 (9)
C3—C4	1.363 (9)	C8—C9	1.498 (8)
C3—H3	0.9300	C9—H9A	0.9600
C4—C5	1.370 (10)	C9—H9B	0.9600
C4—Cl1	1.753 (6)	C9—H9C	0.9600
C5—C6	1.380 (9)	N1—H1N	0.88 (3)
C5—H5	0.9300	N2—H2N	0.87 (3)
C6—H6	0.9300		
C2—C1—C6	120.3 (6)	N1—C7—N2	116.9 (6)
C2—C1—N1	118.5 (6)	N1—C7—S1	125.2 (5)
C6—C1—N1	121.1 (6)	N2—C7—S1	117.9 (5)
C1—C2—C3	119.1 (6)	O1—C8—N2	121.8 (6)
C1—C2—H2	120.4	O1—C8—C9	123.9 (6)
C3—C2—H2	120.4	N2—C8—C9	114.0 (6)
C4—C3—C2	120.2 (6)	C8—C9—H9A	109.5
C4—C3—H3	119.9	C8—C9—H9B	109.5
C2—C3—H3	119.9	H9A—C9—H9B	109.5
C3—C4—C5	120.6 (6)	C8—C9—H9C	109.5
C3—C4—Cl1	119.4 (6)	H9A—C9—H9C	109.5
C5—C4—Cl1	120.0 (5)	H9B—C9—H9C	109.5
C4—C5—C6	119.9 (6)	C7—N1—C1	124.8 (5)
C4—C5—H5	120.1	C7—N1—H1N	122 (4)
C6—C5—H5	120.1	C1—N1—H1N	112 (4)
C5—C6—C1	119.8 (7)	C8—N2—C7	128.0 (6)
C5—C6—H6	120.1	C8—N2—H2N	121 (4)
C1—C6—H6	120.1	C7—N2—H2N	110 (4)
C6—C1—C2—C3	−0.8 (10)	N1—C1—C6—C5	−178.9 (6)
N1—C1—C2—C3	178.0 (6)	N2—C7—N1—C1	178.1 (6)
C1—C2—C3—C4	2.1 (11)	S1—C7—N1—C1	−3.6 (10)
C2—C3—C4—C5	−2.3 (12)	C2—C1—N1—C7	122.7 (7)
C2—C3—C4—Cl1	177.1 (5)	C6—C1—N1—C7	−58.6 (10)
C3—C4—C5—C6	1.2 (12)	O1—C8—N2—C7	7.8 (13)
Cl1—C4—C5—C6	−178.1 (6)	C9—C8—N2—C7	−178.0 (7)
C4—C5—C6—C1	0.0 (11)	N1—C7—N2—C8	−6.1 (11)
C2—C1—C6—C5	−0.2 (11)	S1—C7—N2—C8	175.5 (6)

Hydrogen-bond geometry (Å, º)

D—H···*A*	*D*—H	H···*A*	*D*···*A*	*D*—H···*A*
N1—H1*N*···O1	0.88 (3)	2.04 (6)	2.662 (7)	128 (6)
N1—H1*N*···O1^{i}	0.88 (3)	2.59 (5)	3.319 (7)	141 (6)
N2—H2*N*···S1^{ii}	0.87 (3)	2.54 (3)	3.379 (6)	163 (6)

Symmetry codes: (i) −*x*+1, −*y*+1, *z*; (ii) −*x*+2, −*y*+1, *z*.